

Electronic supplementary information for:

Cis or Trans with class II diterpene cyclases[†]

Meirong Jia and Reuben J. Peters*

*Roy J. Carver Department of Biochemistry, Biophysics & Molecular Biology, Iowa State University, Ames, IA 50010 (*E-mail: rjpeters@iastate.edu)*

Table of Contents

S1-3	Experimental methods
S3	Table S1. Class II diterpene cyclases (DTCs) used in this study.
S4	Figure S1. The structure of (13 <i>Z</i>)- <i>cis-syn</i> -copalol, 4' with numbering and selective correlations used to assign the structure.
S4	Table S2. NMR data for ¹ H and ¹³ C chemical shifts of 4' (CDCl ₃ , 800 MHz).
S5	Figure S2. ¹ H NMR spectrum of 4' .
S5	Figure S3. ¹³ C NMR spectrum of 4' .
S6	Figure S4. ¹ H- ¹ H COSY spectrum of 4' .
S6	Figure S5. HSQC spectrum of 4' .
S7	Figure S6. HMBC spectrum of 4' .
S7	Figure S7. HMQC-COSY spectrum of 4' .
S8	Figure S8. NOESY spectrum of 4' .
S8	Chart S1. Comparison of known DTC products from 1 and putative products from 2 .
S9	References

Experimental methods

General

Unless otherwise noted, chemicals were purchased from Fisher Scientific and molecular biology reagents from Invitrogen. The modularity of the metabolic system utilized here is based on the use of DEST cassettes that enable facile recombination via the Gateway cloning system (Invitrogen).¹ Production of **1** relies on a GGPP synthase expressed from a pACYCDuet (Novagen) based expression vector pGG, which also has been further modified with the addition of a DEST cassette, pGG-DEST, into which the DTCs utilized here were recombined from pENTR/SD/D-TOPO vectors. Production of **2** was accomplished with a previously reported pEXP5-CT-TOPO-based NNPP synthase (SINNPS) expression construct,² which was further modified by insertion of a DEST cassette into which each of the twelve DTCs utilized here were recombined.³ All constructs were verified by full sequencing of the inserted gene.

Metabolic Engineering

All metabolic engineering was carried out using the *E. coli* OverExpress C41 strain (Lucigen). For production of **1** or **2**, DTC constructs with either AgGGPS or SINNPS were co-transformed with pIRS, which overexpresses key enzymes from the endogenous

isoprenoid precursor supply pathway, leading to increased flux to terpenoids.⁴ For initial activity screening purpose, recombinant cultures were grown in 50 mL TB medium (pH = 7.0), with appropriate antibiotics, in 250 mL Erlenmeyer flasks. These cultures were first grown at 37 °C to mid-log phase ($OD_{600} \sim 0.7$), then the temperature dropped to 16 °C for 0.5 h prior to induction with 1 mM isopropylthiogalactoside (IPTG) and supplementation with 40 mM pyruvate and 1 mM $MgCl_2$. The induced cultures were grown for an additional 72 h before extraction with an equal volume of hexanes, with the organic phase then separated, and concentrated under N_2 when necessary.

Diterpene product analysis by GC-MS chromatography

Gas chromatography with mass spectral detection was carried on a Varian 3900 GC with a Saturn 2100T ion trap mass spectrometer in electron ionization (70 eV) mode, using an Agilent HP-5MS column (Agilent, 19091S-433) with 1.2 mL/min helium flow rate. Samples (1 μ L) were injected in splitless mode by an 8400 autosampler with the injection port set at 250 °C. The following temperature program was used: the column oven temperature initially started at 50 °C, which was maintained for 3 min, and then increased at a rate of 15 °C/min to 300 °C, where it was held for another 3 min. Mass spectrum was recorded by mass-to-charge ratio (m/z) values in a range from 90 to 650, starting from 13 min after sample injection until the end of the run.

Diterpene production and purification

To obtain sufficient amount of new enzymatic products for NMR analysis, the bacterial cultures described above were simply scaled up to 2 x 1 L in 2.8 L Fernbach flasks. All other procedures were identical except that the extraction was repeated twice to ensure full yield. The pooled separated organic phase was dried by rotary evaporation under vacuum, and the residue was re-suspended in 5 mL hexane for subsequent fractionation via flash chromatography over a 4 g-silica column (Grace) using a Grace Reveleris flash chromatography system with UV detection and automated injector and fraction collector, run at 15 mL/min. Briefly, the column was pre-equilibrated with hexanes and the sample injected, followed by 100% hexane (0-4 min), 0-100% acetone (4-5 min), 100% acetone (5-8 min), with peak-based fraction collection (15 mL maximum per tube). The oxygen-containing products generally eluted in the 100% acetone fractions. Fractions of interest were dried under N_2 , re-suspended in 2 mL methanol, and filtered through 0.2 μ m cellulose filter (Thermo scientific). These fractions were further separated using an Agilent 1200 series HPLC instrument equipped with a diode array UV detector and automated injector and fraction collector, over an analytical C-8 column (Kromasil[®] C8, 50 \times 4.6 mm) run at 0.5 mL/min, the following elution program was applied. After pre-equilibration of the column with acetonitrile/water (1:1), the sample was injected, followed by washing (0-2 min) with same acetonitrile/water mix, then the percentage of acetonitrile increased to 100% (2-10 min), and final elution with 100% acetonitrile (10-30 min), with collection of 0.5 mL fractions. These were analyzed by GC-MS, those containing pure **4'** were pooled, dried under N_2 , and weighed, with a final yield of \sim 6 mg. This material was then dissolved in 0.5 mL deuterated $CDCl_3$ (Aldrich) for NMR analysis.

Chemical structure identification by NMR analysis

NMR analysis was carried out at 25 °C on a Bruker AVIII-800 spectrometer equipped with a 5-mm HCN cryogenic probe, using TopSpin 3.2 software. Chemical shifts were calculated by reference to CDCl₃ (¹³C 77.23 ppm, ¹H 7.24 ppm) signals offset from TMS. All spectra were acquired using standard programs from the TopSpin 3.2 software, with collection of 1D ¹H-NMR, and 2D double-quantum filtered correlation spectroscopy (DQF-COSY), heteronuclear single-quantum coherence (HSQC), heteronuclear multiple-bond correlation (HMBC), HMQC-COSY and NOESY (800 MHz), as well as 1D ¹³C-NMR (201 MHz) spectra. Observed HMBC correlations were used to propose a partial structure, while COSY correlations between protonated carbons were used to complete the structure, which was further verified by HSQC correlations. Observed correlations from NOESY spectrum were used to assign the relative stereochemistry of chiral carbons and also the configuration of double bonds, where applicable.

Chemical structure identification by optical rotation measurement

To investigate the absolute configuration of compound **4'**, its optical rotation was measured in CHCl₃ solvent on a JASCO model DIP-370 digital polarimeter at 25 °C. The measurement was carried out according to the instruction manual, in particular using mode 1 with tube E (50 mm). The instrument was blanked with pure solvent, and 5 readings for each sample were recorded and the average value reported here.

Table S1. Class II diterpene cyclases (DTCs) used in this study.

DTC	Origin	Product ^a	Reference
AgAS:D621A ^b	<i>Abies grandis</i>	copalyl diphosphate (CPP, 3)	5
ZmCPS2/An2	<i>Zea mays</i>	<i>ent</i> -CPP	6
OsCPS4	<i>Oryza sativa</i>	<i>syn</i> -CPP	7
SmCPS/KSL1: D501A/D505A ^b	<i>Selaginella moellendorffii</i>	<i>endo</i> -CPP (5)	8
NgCLS	<i>Nicotiana glutinosa</i>	8 α -hydroxy-CPP (7)	9
AtCPS:H263A ^c	<i>Arabidopsis thaliana</i>	8 β -hydroxy- <i>ent</i> -CPP	10
KgTPS	<i>Kitasatospora griseola</i>	<i>syn</i> -kolavenyl diphosphate	11
MtHPS	<i>Mycobacterium tuberculosis</i>	halimadienyl diphosphate (9)	12
MvCPS1	<i>Marrubium vulgare</i>	peregrinol diphosphate	13
AtCPS:H263Y ^d	<i>Arabidopsis thaliana</i>	<i>ent</i> -kolavenyl diphosphate	14
Haur_2145	<i>Herpetosiphon aurantiacus</i>	kolavenyl diphosphate	15
OsCPS4:H501D ^d	<i>Oryza sativa</i>	<i>syn</i> -halimadienyl diphosphate	16

^aPreviously assigned common names.

^bMutation(s) that blocks class I DTS activity of this bifunctional DTC/DTS.

^cMutant with hydrolyase activity.

^dMutant that yields rearranged product.

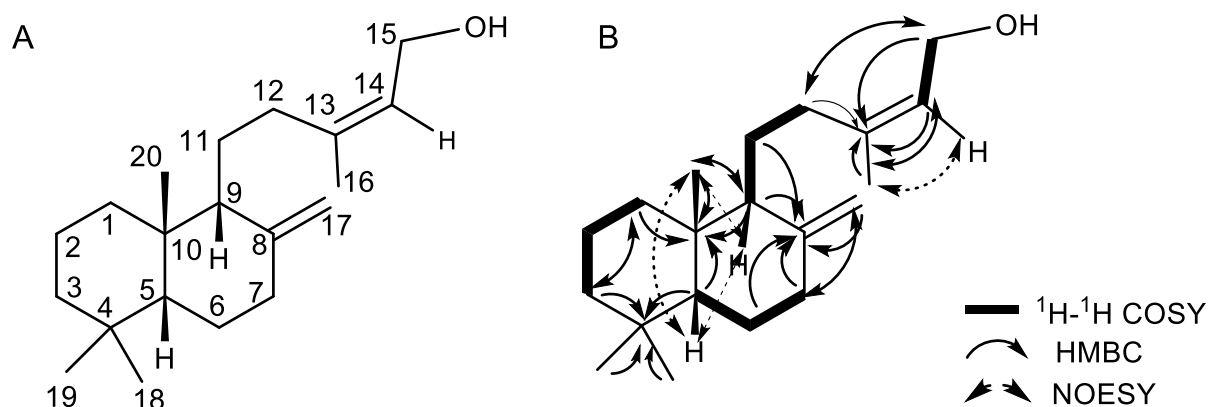


Figure S1. The structure of **4'** with number and selective correlations used to assign the structure. (A) Numbering. (B) ^1H - ^1H COSY correlations, selected HMBC correlations and NOESY Nuclear Overhauser Effect dipole-dipole correlations used to assign the structure.

Table S2. NMR data for ^1H and ^{13}C chemical shifts of **4'** (CDCl_3 , 800 MHz).

Position	(13Z)- <i>cis-syn</i> -copalol (4')	
	δ_{H}	δ_{C}
1 a	1.76 (1H, m)	39.2
b	1.02 (1H, td, $J = 13.1, 4.2$ Hz)	
2 a	1.59 (1H, m)	19.6
b	1.51 (1H, m)	
3 a	1.42 (1H, m)	42.3
b	1.21 (1H, td, $J = 13.4, 4.2$ Hz)	
4		33.8
5	1.11 (1H, dd, $J = 12.7, 2.9$ Hz)	55.7
6 a	1.75 (1H, m)	24.7
b	1.35 (1H, m)	
7 a	2.43 (1H, m)	38.5
b	1.99 (1H, td, $J = 13.0, 4.8$ Hz)	
8		148.8
9	1.58 (1H, m)	56.0
10		39.8
11 a	1.62 (1H, m)	21.9
b	1.46 (1H, m)	
12 a	2.11 (1H, d, $J = 6.5$ Hz)	30.7
b	2.10 (1H, d, $J = 6.5$ Hz)	
13		140.9
14	5.46 (1H, t, $J = 7.1$ Hz)	124.7
15	4.10 (2H, m)	59.3
16	1.77 (3H, s)	23.5
17 a	4.90 (1H, d, $J = 1.5$ Hz)	106.6
b	4.59 (1H, d, $J = 1.5$ Hz)	
18	0.90 (3H, s)	33.8
19	0.83 (3H, s)	21.9
20	0.71 (3H, s)	14.8

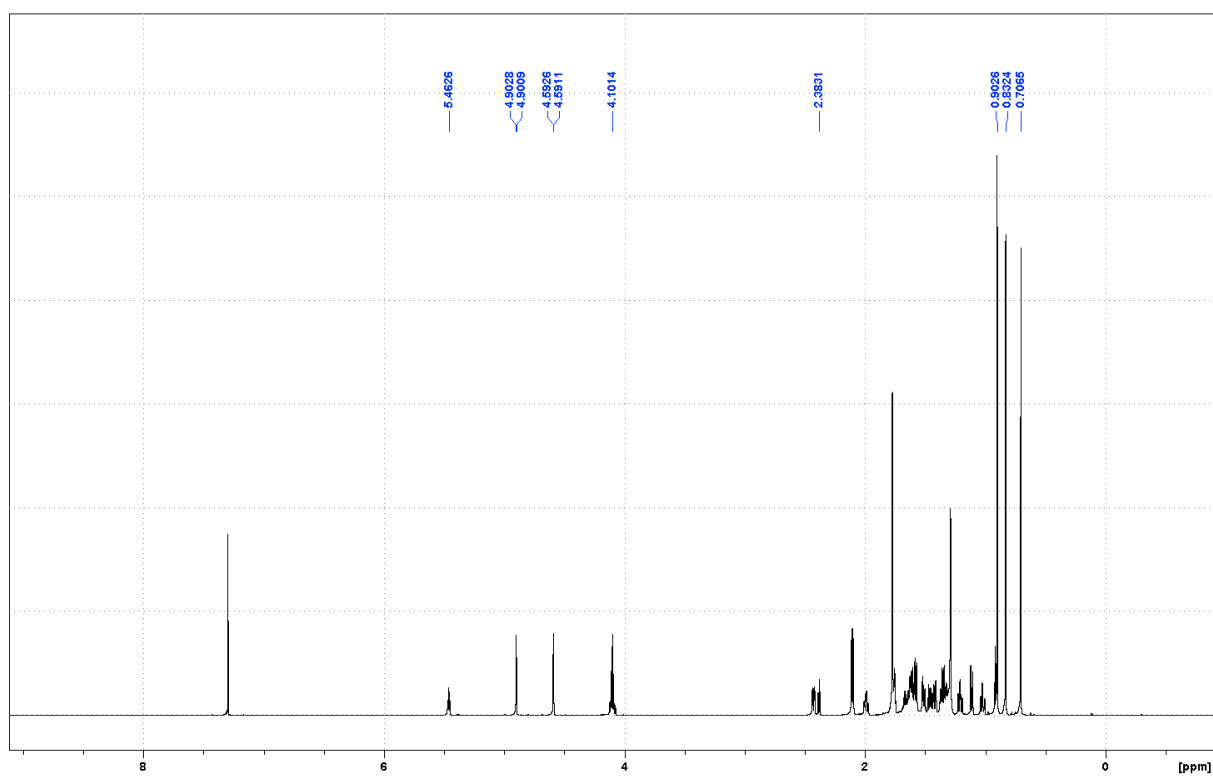


Figure S2. ¹H NMR spectrum of 4'.

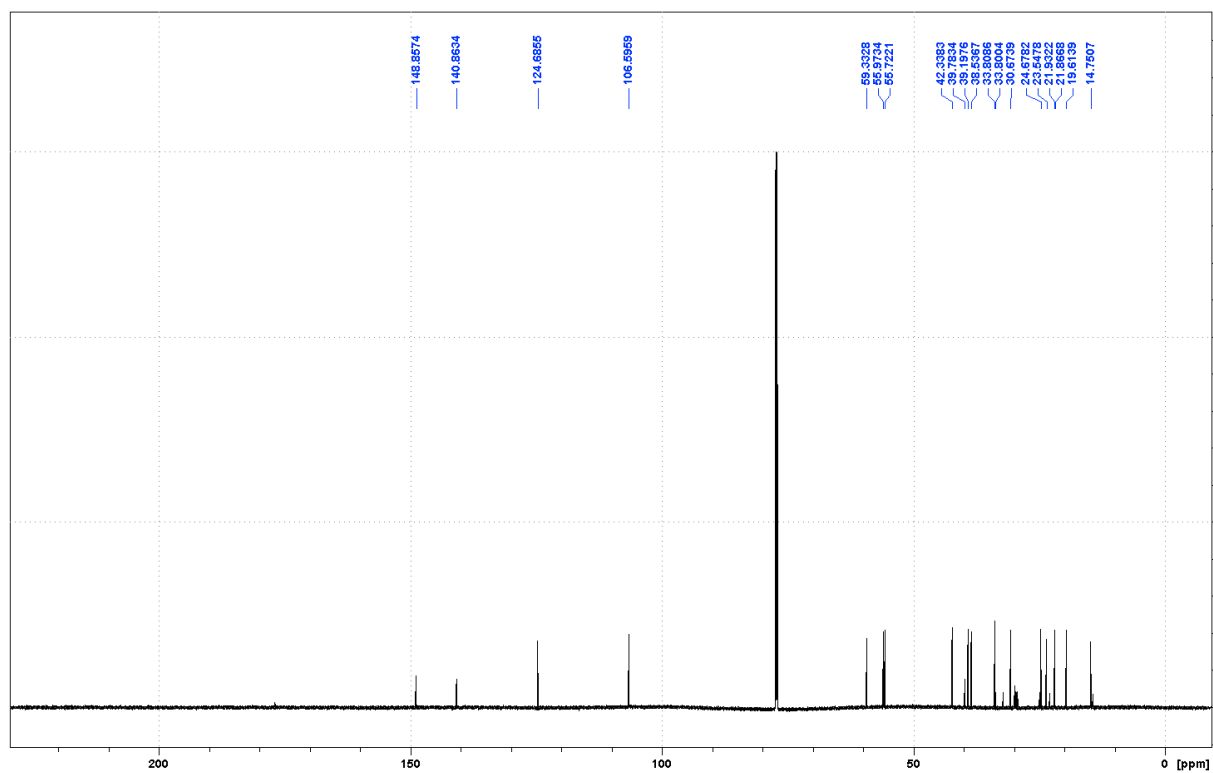


Figure S3. ¹³C NMR spectrum of 4'.

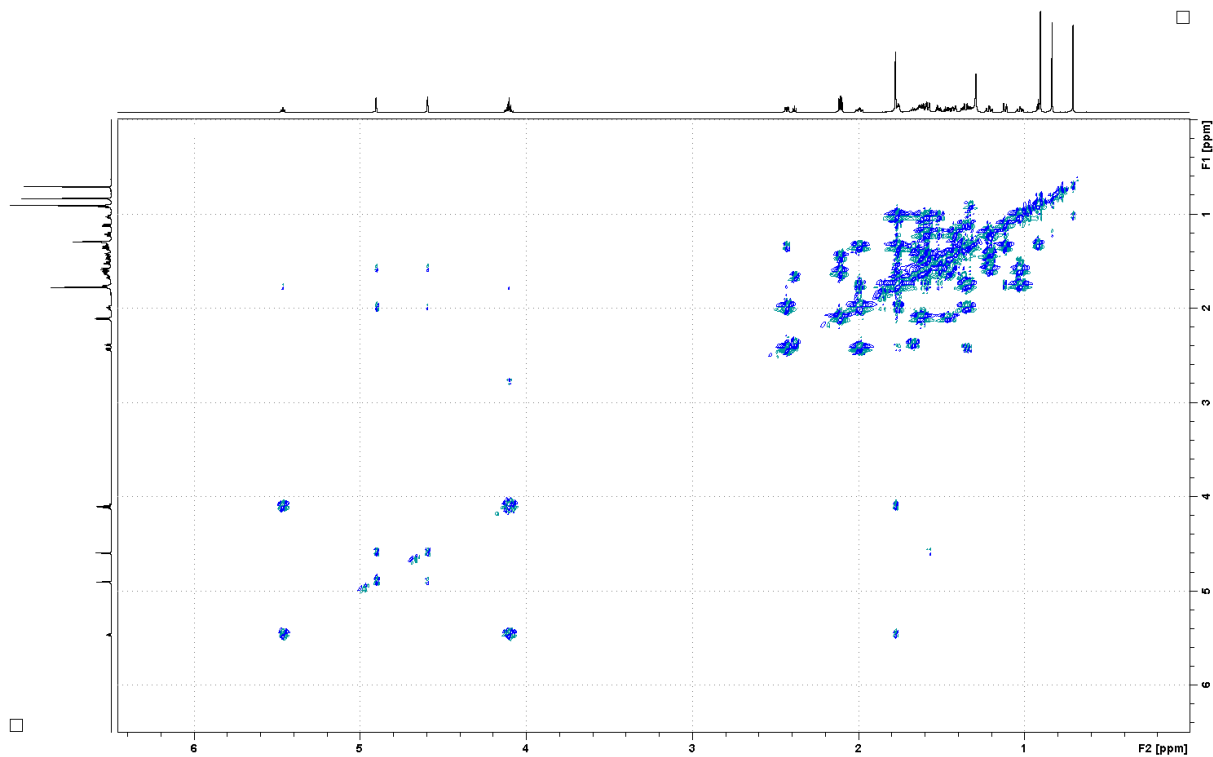


Figure S4. ^1H - ^1H COSY spectrum of 4'.

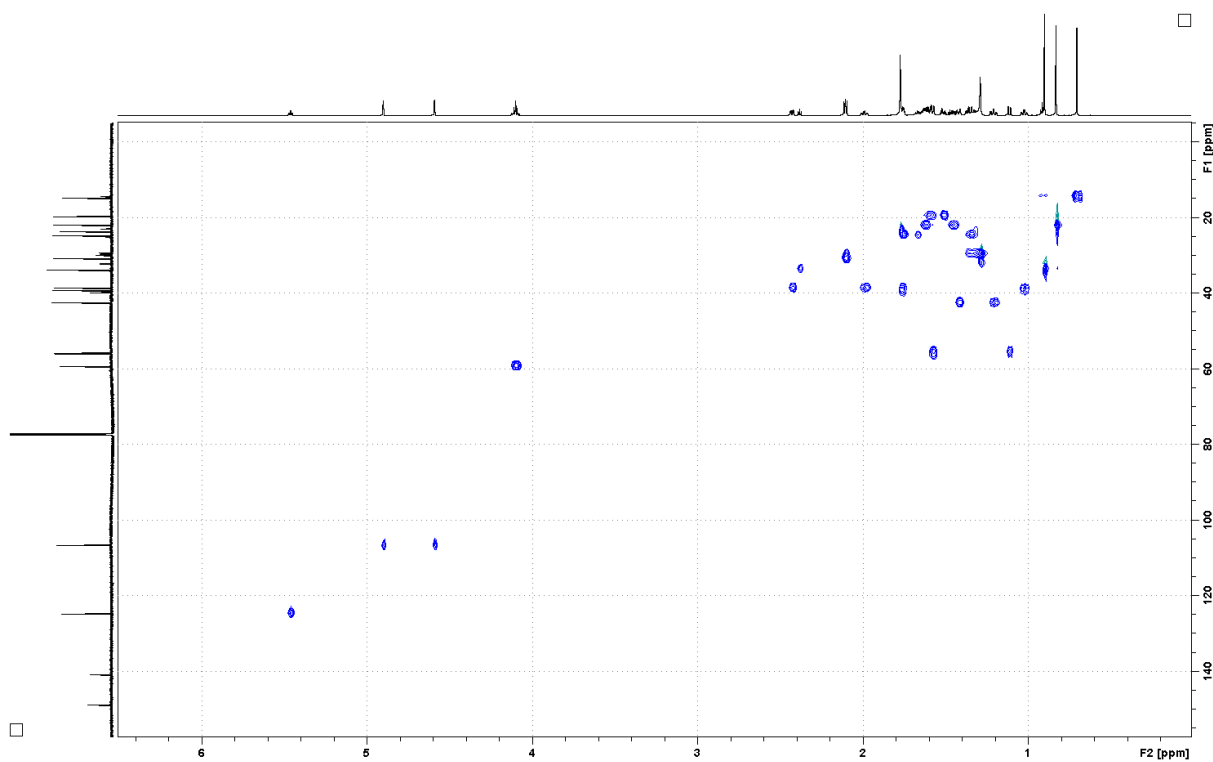


Figure S5. HSQC spectrum of 4'.

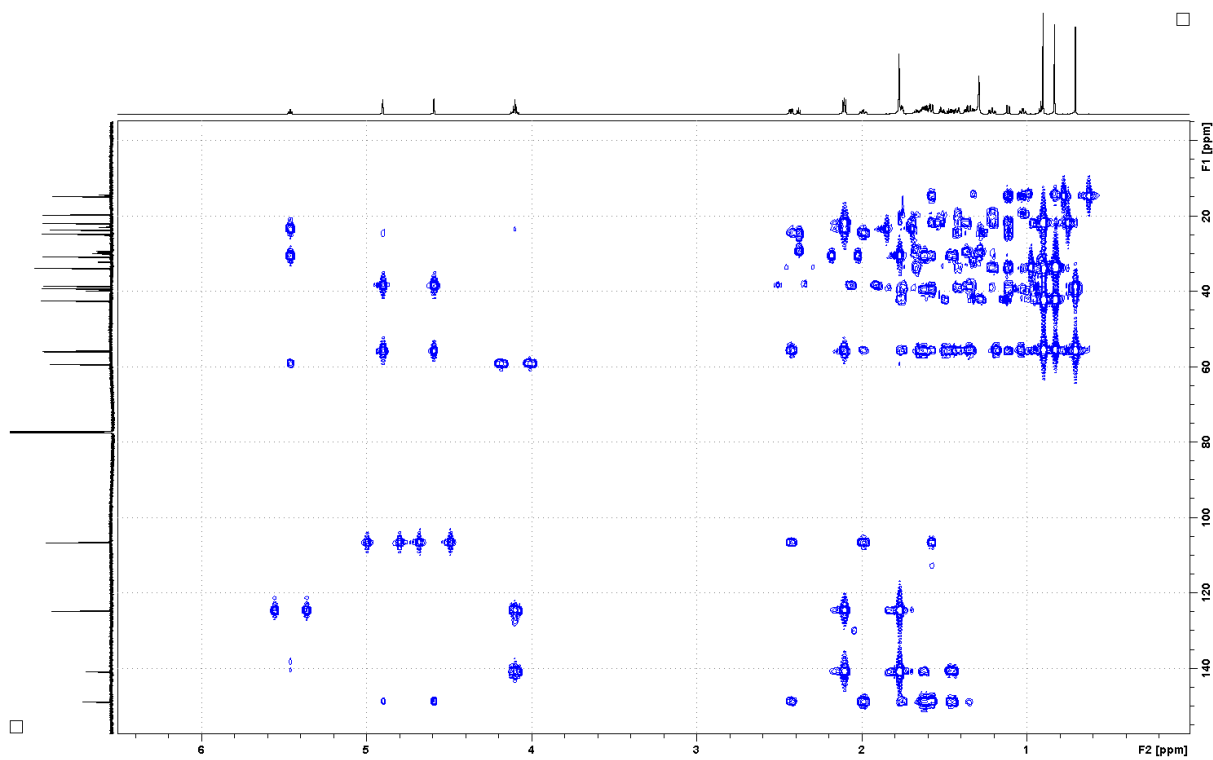


Figure S6. HMBC spectrum of 4'.

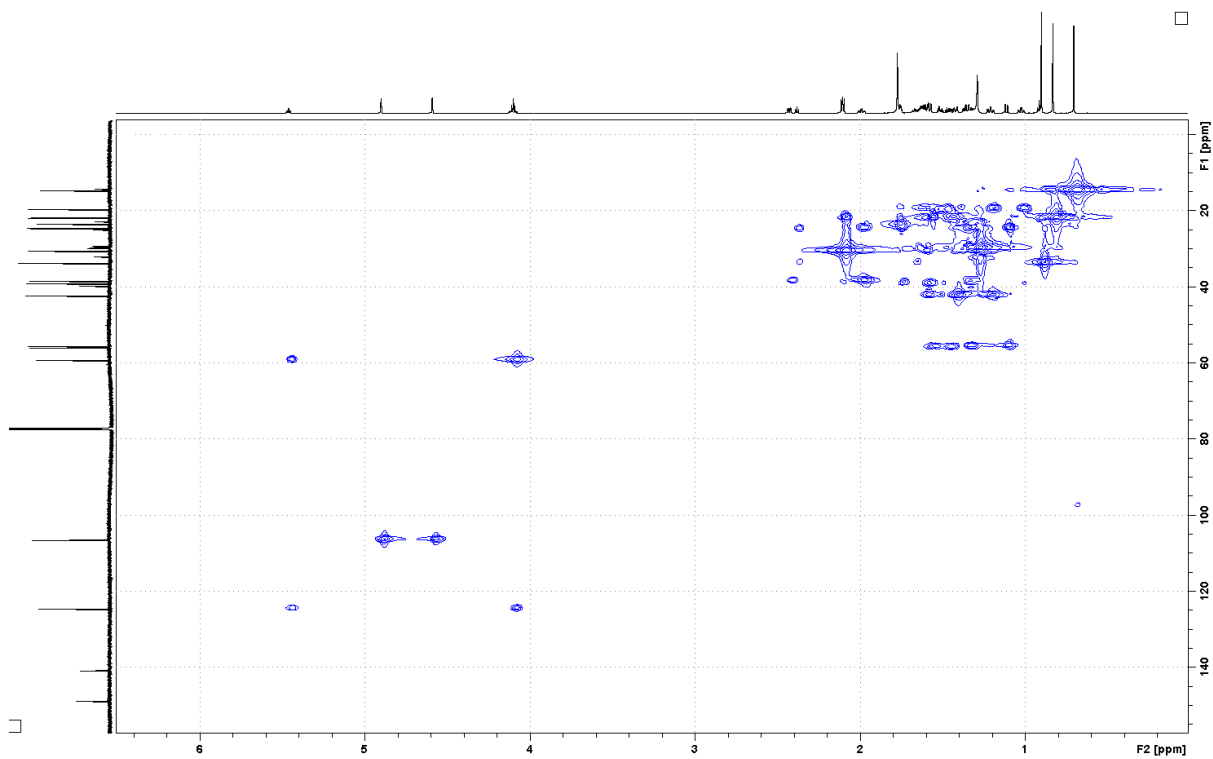


Figure S7. HMQC-COSY spectrum of 4'.

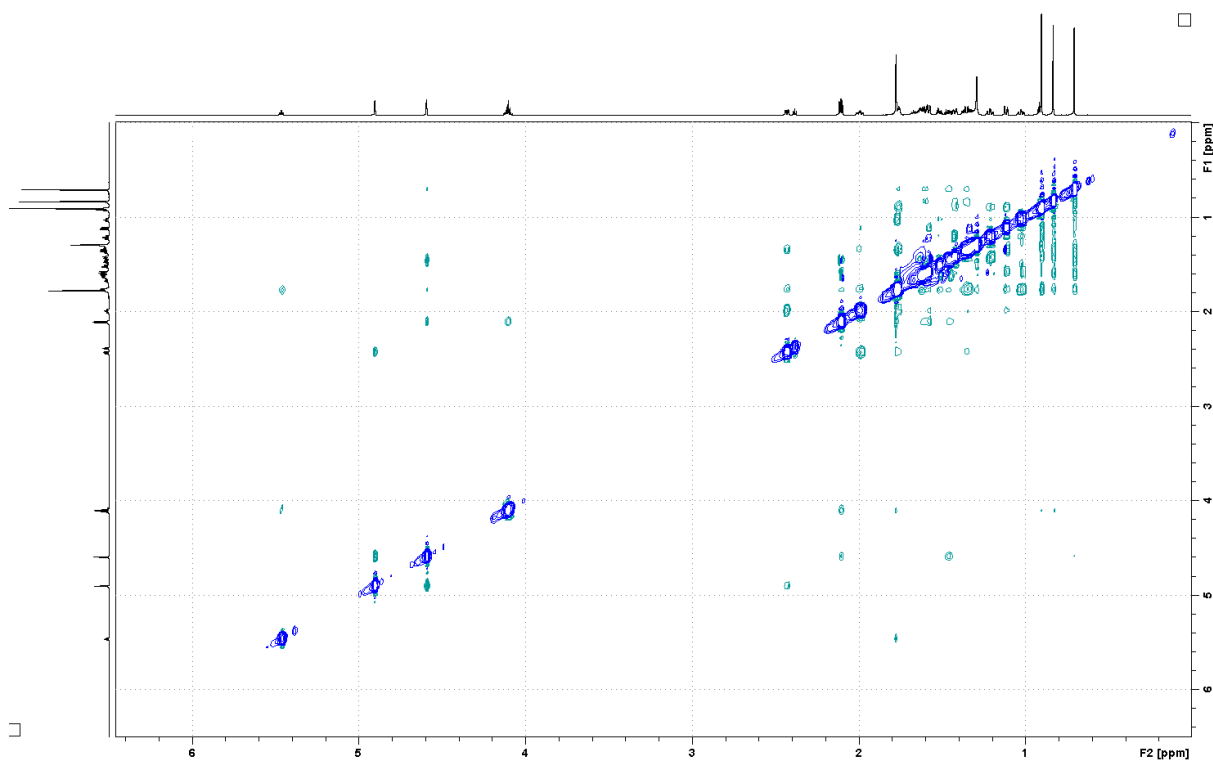


Figure S8. NOESY spectrum of **4'**.

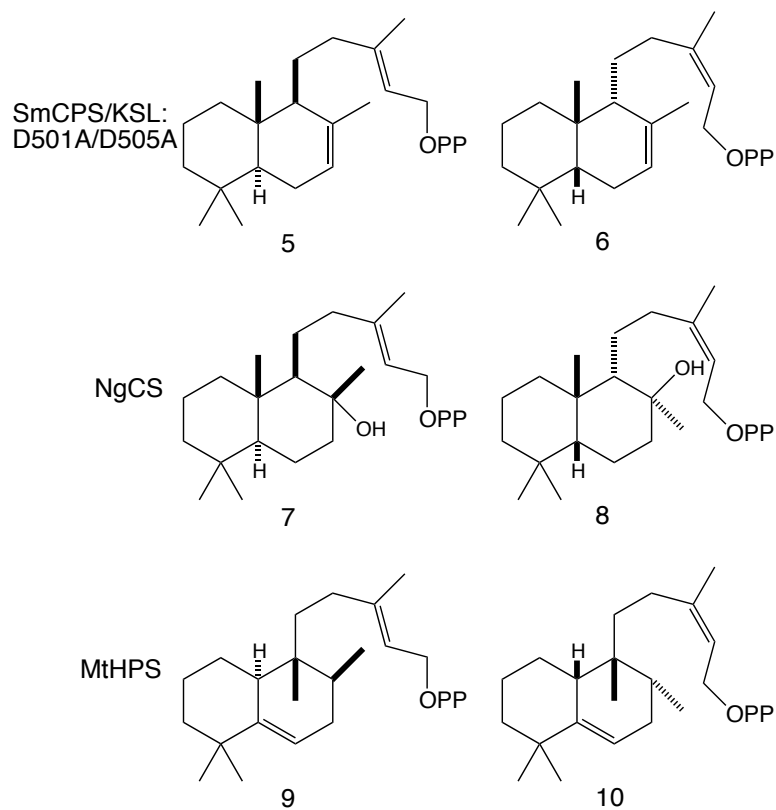


Chart S1. Comparison of known DTC products from **1** and putative products from **2**. DTC indicated on left, with known product from **1** in middle, and putative product from **2** on the right (numbering as defined in the manuscript).

References:

1. A. Cyr, P. R. Wilderman, M. Determan and R. J. Peters, *J. Am. Chem. Soc.*, 2007, **129**, 6684-6685.
2. J. Zi, Y. Matsuba, Y. Hong, A. Jackson, E. Pichersky, D. J. Tantillo and R. J. Peters, *J. Am. Chem. Soc.*, 2014, **136**, 16951-16953.
3. M. Jia, K. C. Potter and R. J. Peters, *Metabolic engineering*, 2016, **37**, 24-34.
4. D. Morrone, L. Lowry, M. K. Determan, D. M. Hershey, M. Xu and R. J. Peters, *Appl. Microbiol. Biotechnol.*, 2010, **85**, 1893-1906.
5. R. J. Peters, J. E. Flory, R. Jetter, M. M. Ravn, H. J. Lee, R. M. Coates and R. B. Croteau, *Biochemistry*, 2000, **39**, 15592-15602.
6. L. J. Harris, A. Sapano, A. Johnston, S. Pristic, M. Xu, S. Allard, A. Kathiresan, T. Ouellet and R. J. Peters, *Plant Mol Biol*, 2005, **59**, 881-894.
7. M. Xu, M. L. Hillwig, S. Pristic, R. M. Coates and R. J. Peters, *The Plant journal : for cell and molecular biology*, 2004, **39**, 309-318.
8. S. Mafu, M. L. Hillwig and R. J. Peters, *ChemBioChem*, 2011, **12**, 1984-1987.
9. J. Criswell, K. Potter, F. Shephard, M. H. Beale and R. J. Peters, *Organic letters*, 2012, **14**, 5828-5831.
10. K. Potter, J. Criswell, J. Zi, A. Stubbs and R. J. Peters, *Angewandte Chemie*, 2014, **53**, 7198-7202.
11. Y. Hamano, Y. Kuzuyama, N. Itoh, K. Furihata, H. Seto and T. Dairi, *J. Biol. Chem.*, 2002, **277**, 37098-37104.
12. F. M. Mann, S. Pristic, H. Hu, M. Xu, R. M. Coates and R. J. Peters, *The Journal of biological chemistry*, 2009, **284**, 23574-23579.
13. P. Zerbe, A. Chiang, H. Dullat, M. O'Neil-Johnson, C. Starks, B. Hamberger and J. Bohlmann, *Plant J*, 2014, **79**, 914-927.
14. K. C. Potter, J. Zi, Y. J. Hong, S. Schulte, B. Malchow, D. J. Tantillo and R. J. Peters, *Angew. Chem. Int. Ed.*, 2016, **55**, 634-638.
15. C. Nakano, M. Oshima, N. Kurashima and T. Hoshino, *Chembiochem*, 2015, **16**, 772-781.
16. K. C. Potter, M. Jia, Y. J. Hong, D. J. Tantillo and R. J. Peters, *Org. Lett.*, 2016, **18**, 1060-1063.